

# 3-D Integrated Electronic Microplate Platform for Low-Cost Repeatable Biosensing Applications

Muneeb Zia, *Student Member, IEEE*, Taiyun Chi, *Student Member, IEEE*,  
 Jong Seok Park, *Student Member, IEEE*, Amy Su, Joe L. Gonzalez, *Student Member, IEEE*,  
 Paul K. Jo, *Student Member, IEEE*, Mark P. Styczynski, Hua Wang, *Senior Member, IEEE*,  
 and Muhamnad S. Bakir, *Senior Member, IEEE*

**Abstract**—This paper presents a 3-D integrated disposable “electronic microplate” (e-microplate) platform that allows the reuse of CMOS biosensor, thereby significantly reducing cost and increasing throughput compared to nondisposable biosensing systems. The e-microplate utilizes mechanically flexible interconnects and through-silicon-vias to electrically connect the cells cultured on the top (sensing electrode side) of the e-microplate to the electrodes on the CMOS biosensor while maintaining a physical separation between the aforementioned substrate tiers. Electrical measurements performed show that the incorporation of the e-microplate does not degrade the sensing amplifier’s gain, 3-dB bandwidth, or the input referred noise; this ensures a high signal-to-noise ratio allowing accurate sensing of weak signals from living cells under test. Cell growth experiments performed show adhesion and growth of mouse embryonic stem cells on the surface of the sensing electrodes of the e-microplate. Impedance mapping for Dulbecco’s phosphate buffered saline solution performed with the e-microplate, for two different e-microplate assemblies, confirms the functional accuracy of the assembled systems.

**Index Terms**—3-D integration, biosensing, disposable, electronic microplate (e-microplate).

## I. INTRODUCTION

CMOS biosensors are increasingly being utilized for sensing various modalities of cellular and molecular samples including, but not limited to, electrical, magnetic, and optical modalities at low cost. Sensing these modalities involves correlating the cellular-based physiological events to change in current or voltage that can then be sensed using integrated electrodes [1]–[9]. A change in electrical response can be induced by the administration of a stimulating chemical or biological agent on electroactive samples (cardiac cells and neurons), and any resulting changes in the sensed signal can

Manuscript received June 20, 2016; revised August 31, 2016; accepted October 24, 2016. Date of publication December 1, 2016; date of current version January 6, 2017. Recommended for publication by Associate Editor A. Jain upon evaluation of reviewers’ comments.

M. Zia, T. Chi, J. S. Park, J. L. Gonzalez, P. K. Jo, H. Wang, and M. S. Bakir are with the Department of Electrical and Computer Engineering, Georgia Institute of Technology, Atlanta, GA 30318 USA (e-mail: muneeb.zia@gatech.edu; terrychi@gatech.edu; ysjspark86@gatech.edu; jgonzalez34@gatech.edu; paul.jo@gatech.edu; hua.wang@ece.gatech.edu; muhammad.bakir@mirc.gatech.edu).

A. Su and M. P. Styczynski are with the Department of Chemical and Biomolecular Engineering, Georgia Institute of Technology, Atlanta, GA 30318 USA (e-mail: asu30@gatech.edu).

Color versions of one or more of the figures in this paper are available online at <http://ieeexplore.ieee.org>.

Digital Object Identifier 10.1109/TCMT.2016.2626789

then be studied to determine the drug efficacy or pathogen mechanistic effects [7], [9].

These cell-based sensing techniques require the growth of cells onto the biosensor’s surface; both the successful adhesion and growth of these cells onto the biosensor are pivotal for meaningful sensing and are strongly affected by the type of material and the surface roughness [10]–[16]. Growth of human cells on a multimodality CMOS biosensor has been shown in [17]. However, growing cells directly onto the biosensor is tedious due to the surface treatments required to enhance biocompatibility and culture cells. Additionally, culturing cells directly onto the CMOS biosensor may be expensive because it is difficult to reuse as it must undergo a rigorous cleansing process or disposed of to avoid contamination [7], [18]. Moreover, even after cleaning and sterilizing the CMOS biosensor surface, the biosensor might not be suitable for reuse if the cell type or the biochemical stimulus to be tested are different. Contamination poses a perpetual risk to the proper functionality of the CMOS biosensor. Furthermore, any electrical connections to the board (e.g., wire bonds in [17]) and culture medium sealing (e.g., polydimethylsiloxane (PDMS) sealing in [17]) need to be replaced for a new sample during which there is a high likelihood of damaging the CMOS biosensor and/or interconnects. To address these challenges, this paper presents a 3-D integrated disposable electronic microplate (e-microplate) platform allowing the reuse of the CMOS biosensor and thereby reducing cost and increasing throughput relative to systems that are nondisposable. The platform utilizes mechanically flexible interconnects (MFIs) and through-silicon-vias (TSVs) to electrically interface the sensing electrodes on the CMOS biosensor to the sensing electrodes on the e-microplate while maintaining a physical separation of the biosensors from the cellular samples. Mouse embryonic stem cell seeding experiment shows successful cell attachment and growth on the sensing electrodes of the e-microplate. The electrical characterization results show that the integration of the e-microplate does not adversely affect the performance of the underlying CMOS biosensor, as seen via the consistency of the internal amplifier gain and the input referred noise. Additionally, the e-microplate system is shown to perform successful impedance mapping on Dulbecco’s phosphate buffered saline (DPBS) solution. The average measured resistance of the TSV-MFI link is 163 mΩ, while the measured 3-dB bandwidth and the integrated input referred noise with the e-microplate included is 0.5–400 Hz

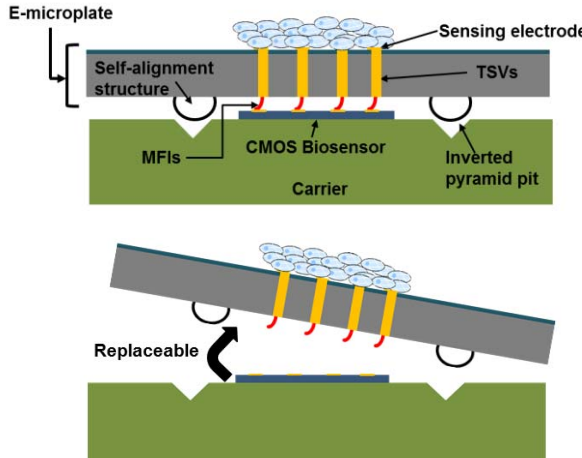


Fig. 1. Envisioned microfabricated e-microplate platform—the e-microplate can be replaced and the biosensor reused.

and  $4.96 \mu\text{V}_{\text{rms}}$ , respectively. The low input noise ensures high signal-to-noise ratio (SNR) for sensing minute biological signals from the cellular samples, which is critical for reliable analysis.

## II. SYSTEM OVERVIEW

Fig. 1 shows the envisioned e-microplate platform. The e-microplate serves as a 3-D integrated disposable tier separating the CMOS biosensor from the cultured cells. Mechanical self-alignment structures and pyramid pits with submicrometer alignment accuracy [18] have been incorporated into this platform to enable low-cost and high-accuracy alignment between the e-microplate and the CMOS biosensor. The gap between the two tiers can be modulated by adjusting the size of the pyramid pits and the self-alignment structures. Electrical interconnections between the cultured cells and the sensing electrodes on the CMOS biosensor are enabled using TSVs and MFI integration. The flexible interconnects compensate for any surface nonplanarity or minor gap variations between tiers while maintaining good electrical connection. After performing required measurements on a cell culture, the e-microplate can be replaced and the CMOS biosensor and board reused for a new set of measurements. The CMOS biosensor presented in [17] was utilized for the e-microplate assembly.

## III. FABRICATION OF E-MICROPLATE

Fig. 2 shows the fabrication process of the e-microplate. The sensing electrodes were fabricated on the top of the e-microplate by the deposition of Ti/Cu/Au using an evaporation process, followed by a subsequent lift-off process. After the formation of the sensing electrodes, gold passivated NiW MFIs, described in [19], were fabricated at the bottom; utilizing NiW to fabricate the MFIs allows for larger deformation within the elastic region owing to its higher yield strength relative to copper [19]. The gold passivation using electroless plating ensures reliable gold-to-gold contact between the MFI and the sensing electrode on the CMOS biosensor. The surface profile of the sensing electrodes for the fabricated e-microplate is shown in Fig. 3. Surface variations and dishing are seen owing to the chemical-mechanical polishing process. Key dimensions of the TSVs

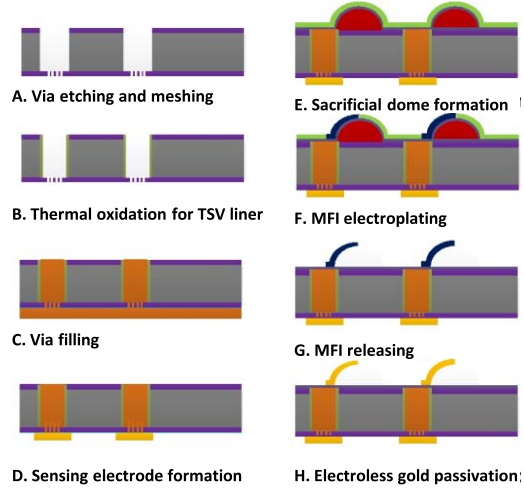


Fig. 2. Fabrication flow of the e-microplate.

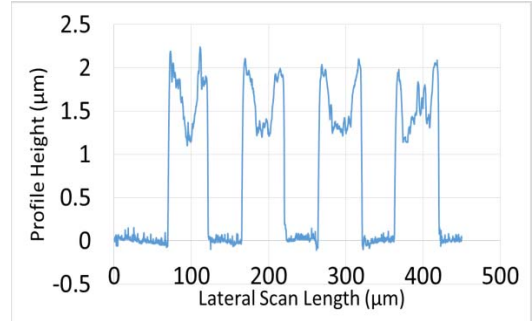
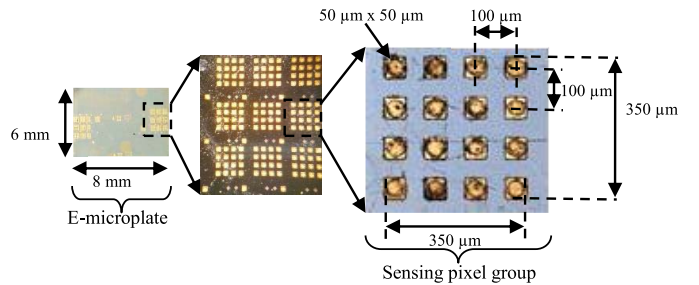


Fig. 3. Sensing pixel group of e-microplate and its surface profile.

and MFIs fabricated for the e-microplate are summarized in Table I. The layout of the e-microplate pixel group was designed to complement the sensor pixel layout on the CMOS biosensor, as described in [17]. Fig. 4 shows an X-ray and an SEM image of the TSV-MFI integration. As seen from the X-ray image, the fabricated TSVs are free of any voids enabling reliable interconnections, which are crucial for the accurate functionality of the platform. The SEM image shows the fabricated MFIs in a pixel group at the bottom of the e-microplate (facing the CMOS biosensor); each pixel group consists of 16 MFIs, which make a contact with the corresponding electrodes on the CMOS biosensor.

## IV. CHARACTERIZATION

### A. Mechanical Characterization of MFIs

Fig. 5 shows the mechanical compliance measurements performed for the MFIs on the e-microplate using a nanoindenter. The  $30\text{-}\mu\text{m}$ -tall MFIs regain their original height after

TABLE I  
DIMENSIONS OF THE FABRICATED MFIS AND TSVS

	Dimension	Value ( $\mu\text{m}$ )
TSVs	Diameter	50
	Height	300
	Pitch	100
MFIs	Thickness	3.5
	Vertical Height	30
	Pitch	100

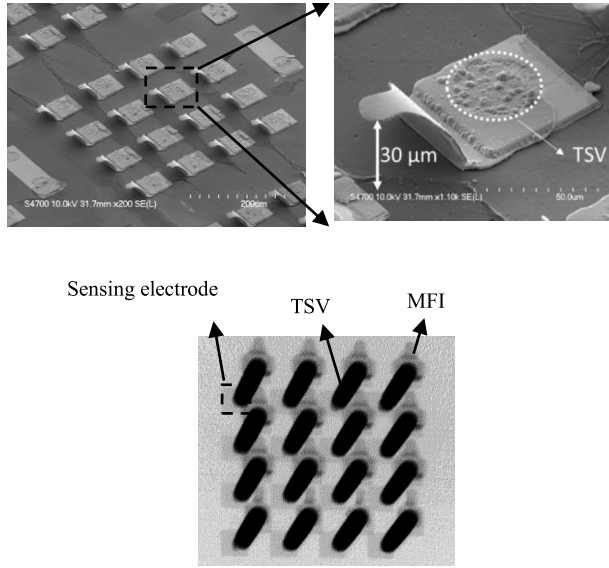


Fig. 4. SEM and X-ray images of the fabricated e-microplate pixel group.

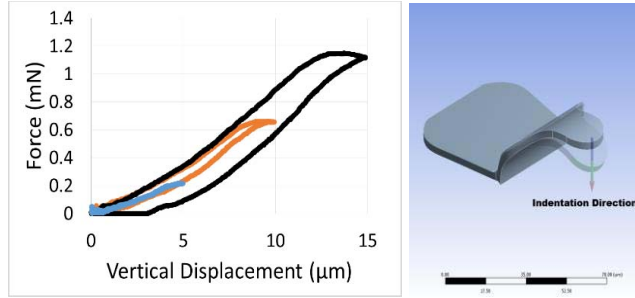


Fig. 5. Mechanical compliance measurements for fabricated MFIs.

up to  $10 \mu\text{m}$  of vertical displacement; this allows them to compensate for minor surface profile or intertier gap variations ensuring a good electrical interconnection to the electrodes on the CMOS biosensor. The measured compliance for the fabricated MFIs is  $\sim 15 \text{ mm/N}$ .

#### B. Electrical Characterization of TSV-MFI Link

Four-point resistance measurement for the TSV-MFI link was carried out by bonding e-microplate, as shown in Fig. 6. The average resistance measured for the link was  $163 \text{ m}\Omega$ , which included the contact resistance. The low value of resistance, compared to the input impedance of the amplifier

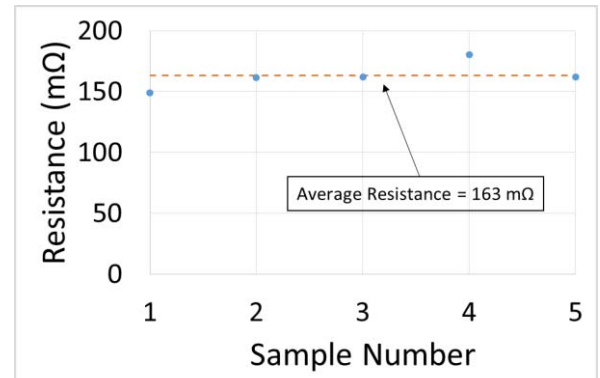
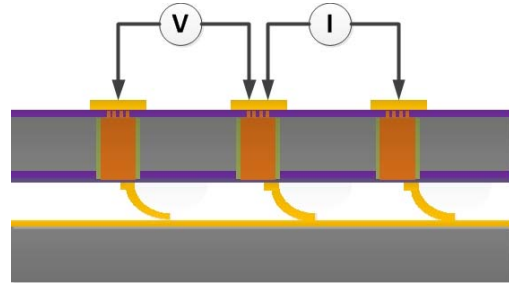


Fig. 6. Four-point resistance measurement results for the TSV-MFI link.

in the CMOS biosensor, ensures negligible signal degradation from the living cells on the sensing electrodes to the biosensor.

#### C. Cell Growth

Cell growth experiments were carried out to verify the viability of mouse stem cell growth on the e-microplate's surface. Attachment and growth of human pluripotent stem cells on oxide surface with gold electrodes and TSVs have been shown in [20].

For the D3 mouse embryonic stem cells growth experiment, the sensing electrodes' surface was first washed with methanol followed by three washes with phosphate-buffered saline. The surface was then gelatin-coated (0.1% gelatin) to promote cell adhesion. The cells were trypsinized with 0.05% trypsin to form a single-cell suspension and seeded at a density of  $70 \text{ k}$  cells/e-microplate in  $400 \mu\text{L}$  of medium. The medium was supplemented with leukemia inhibitory factor to maintain cell pluripotency. Thereafter, the medium was changed every two days, and cell growth monitored by examination with a stereoscope. The results are shown in Table II.

As seen from Table II, the mouse stem cells adhere to the sensing electrodes after 48 h of cell seeding. Subsequent growth is observed after 96 and 144 h of cell seeding, respectively. After the 144-h mark, cells are seen to cover the majority of the sensing electrodes on both the surfaces. This further warrants the utilization of e-microplates for cell-based assays of varying types and makes the platform versatile and adaptable.

#### D. Integrated System Characterization

A twofold system-level characterization was performed for the assembled e-microplate system. First, the CMOS

TABLE II

MOUSE EMBRYONIC STEM CELL GROWTH ON OXIDE AND NITRIDE SURFACES WITH SENSING ELECTRODES

Surface	48 hours	96 hours	144 hours
Oxide			
Nitride			

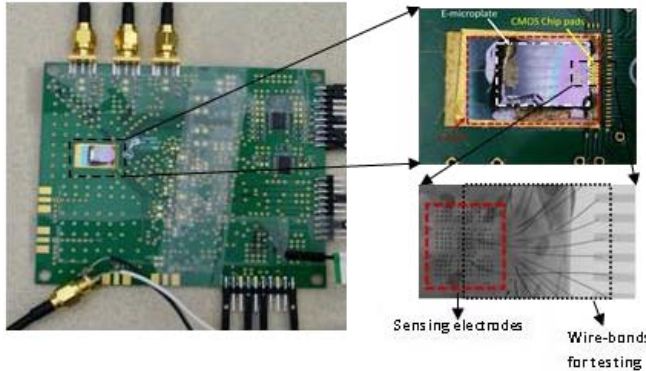


Fig. 7. Test setup for gain and noise measurements—sensing electrodes were wire-bonded to test board for measurements.

biosensor's internal amplifier gain and input referred noise were measured through the e-microplate's TSV-MFI interconnections. Second, impedance mapping of DPBS solution was performed to verify the functional accuracy of two different assembled systems. Fig. 7 shows the assembled e-microplate system used for internal amplifier gain and noise measurements; the system includes the e-microplate, carrier, and CMOS biosensor assembly mounted onto the test board. For impedance mapping, a standard 35-mm Petri dish with a drilled-out bottom was mounted onto the board and sealed using PDMS to provide electrical isolation while maintaining biocompatibility (Fig. 8). Fig. 9 shows the X-ray image of a pixel group in the assembled platform; the MFIs are seen to be well aligned to the sensing electrodes on the CMOS biosensor, ensuring good electrical interconnection.

Fig. 10 shows the circuit schematic for the in-pixel trimodality sensor. For the extracellular potential recording, in-pixel op-amp, pseudoresistors, and capacitors C1 and C2 are configured as a high-pass inverting amplifier with a voltage gain of  $C1/C2$  and a low cutoff frequency of  $1/2\pi R_{pseudo}C2$ . Note that the high cutoff frequency and the voltage gain



Fig. 8. Test setup for impedance mapping.

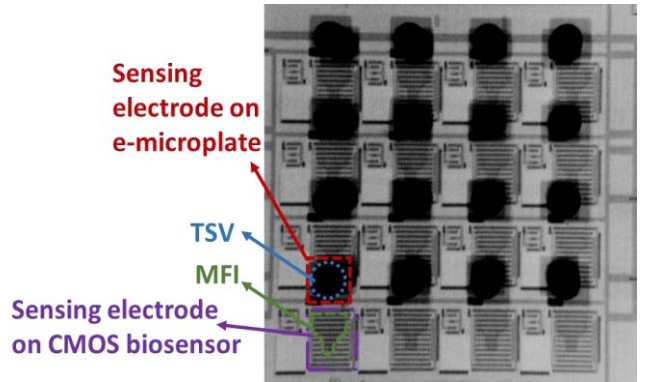


Fig. 9. X-ray image showing accurate alignment between e-microplate and CMOS biosensor.

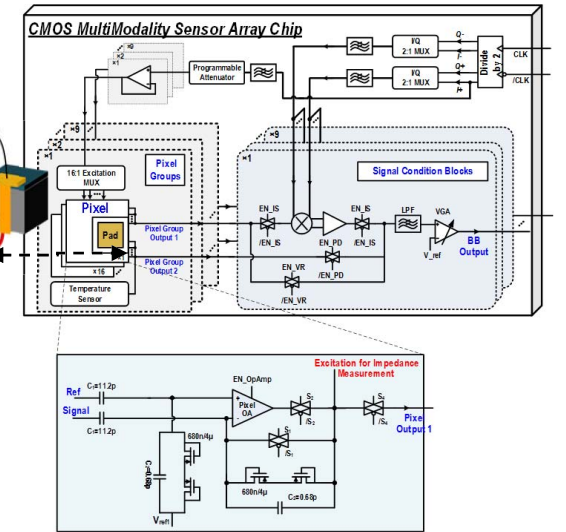


Fig. 10. Schematic of internal voltage sensing amplifier and its connection to the e-microplate's pixel.

are fully programmable in signal conditioning block. For the complex impedance measurement, two pixel electrodes (one for the voltage excitation and the other for the current sensing) are selected through the switch mux, and the generated voltage

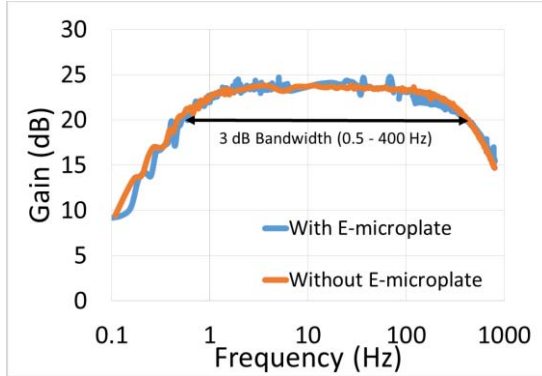


Fig. 11. Amplifier gain measurements—the amplifier gain remains unchanged with the incorporation of the e-microplate.

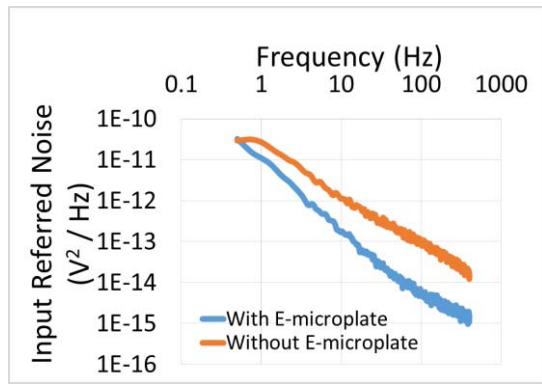


Fig. 12. Input referred noise measurements—low input referred noise ensures high SNR when measuring weak signals.

excitation signals bypass the in-pixel op-amp by enabling the transmission gate switch S1 and are ac-coupled to the voltage excitation electrode. The op-amp in the voltage excitation pixel is switched OFF during the voltage excitation. The resulting current flows through the capacitors C1 and C2 in the selected current sensing pixel and is converted into the voltage at the output of the amplifier. This voltage signal passes the mixer, programmable low-pass filter, and programmable gain amplifier to complete the complex impedance measurement. The quadrature signals are sequentially applied to the mixer for complex impedance measurement.

To test the effect of the e-microplate on the internal amplifier gain and input referred noise, interconnections were made by wire-bonding the sensing electrodes on the e-microplate to the test board; this allowed the test signals to traverse through the TSV-MFI link to the sensing electrode on the CMOS biosensor. Fig. 11 shows the amplifier gain, measured with and without the e-microplate. The results show that the incorporation of the e-microplate does not affect the amplifier gain; also, the 3-dB bandwidth remains unchanged. Similarly, the input referred noise, shown in Fig. 12, does not degrade with the incorporation of the e-microplate; the integrated input referred noise of the amplifier, from 0.5 to 400 Hz, was measured to be  $4.96 \mu\text{V}_{\text{rms}}$ . This low input noise ensures high SNR when measuring extremely weak biological signals from living cells (e.g., cardiac cells or neurons), which is critical in ensuring the integrity of the measured data.

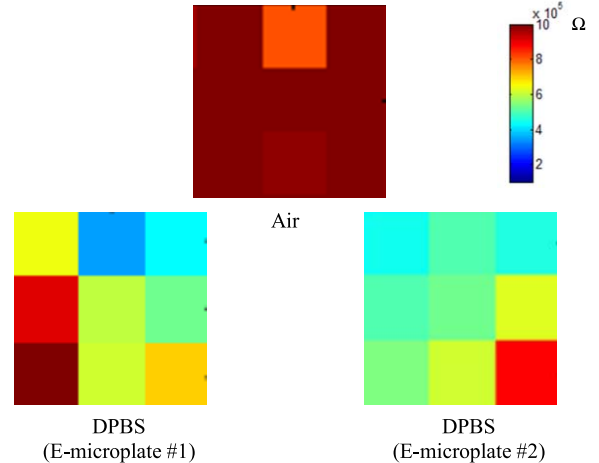


Fig. 13. Impedance measurement for air and DPBS measured via e-microplate's pixel group—measurements verify functional accuracy of the platform.

Impedance mapping, using similar techniques as described in [17], was performed for DPBS for two different e-microplates and compared to air to verify the capability and functional accuracy of the impedance mapping in the e-microplate assembly. The results utilizing the high yield pixels in the e-microplate, shown in Fig. 13, confirm accurate assembly functionality for two different e-microplate assemblies.

## V. CONCLUSION

A low-cost, disposable platform using 3-D IC technology, capable of providing electrical interconnections between living cells and CMOS biosensors, is presented. The e-microplate sits atop the CMOS biosensor circumventing the need for direct cell growth on the CMOS biosensor surface, while the TSV-MFI link provides the necessary electrical interconnections from the cells to the biosensor. The void-free TSVs and the gold passivated NiW MFIs ensure reliable connections to the pixel array on the biosensor, which are essential for accurate sensing. Mouse embryonic stem cells are shown to attach and grow on the sensing electrodes of the e-microplate, warranting it suitable for cell-based assays. The integration of the e-microplate does not degrade the CMOS biosensor's amplifier gain or input referred noise, hence ensuring accurate sensing of weak biological signals from living cells cultured on the e-microplate, which is critical for reliable data analysis. Impedance maps generated for air and DPBS confirm the functional accuracy of the developed platform.

## REFERENCES

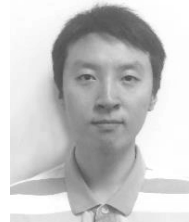
- [1] H. Wang, "Magnetic sensors for diagnostic medicine: CMOS-based magnetic particle detectors for medical diagnosis applications," *IEEE Microw. Mag.*, vol. 14, no. 5, pp. 110–130, Jul. 2013.
- [2] M. Schienle *et al.*, "A fully electronic DNA sensor with 128 positions and in-pixel A/D conversion," *IEEE J. Solid-State Circuits*, vol. 39, no. 12, pp. 2438–2445, Dec. 2004.
- [3] F. Heer, M. Keller, G. Yu, J. Janata, M. Josowicz, and A. Hierlemann, "CMOS electro-chemical DNA-detection array with on-chip ADC," in *IEEE ISSCC Dig. Tech. Papers*, Feb. 2008, pp. 168–604.

- [4] B. Jang, P. Cao, A. Chevalier, A. Ellington, and A. Hassibi, "A CMOS fluorescent-based biosensor microarray," in *IEEE ISSCC Dig. Tech. Papers*, Feb. 2009, pp. 436–437.
- [5] D. Hall, R. S. Gaster, S. J. Osterfeld, K. Makinwa, S. X. Wang, and B. Murmann, "A 256 channel magnetoresistive biosensor microarray for quantitative proteomics," in *Proc. IEEE VLSI Circuits (VLSIC)*, Jun. 2011, pp. 174–175.
- [6] S. Gambini *et al.*, "A CMOS 10kpixel baseline-free magnetic bead detector with column-parallel readout for miniaturized immunoassays," in *IEEE ISSCC Dig. Tech. Papers*, Feb. 2012, pp. 126–128.
- [7] H. Wang, A. Mohdavi, D. Tirrell, and A. Hajimiri, "A magnetic cell-based sensor," *Lab Chip*, vol. 12, no. 21, pp. 4465–4471, 2012.
- [8] H. Wang, S. Kosai, C. Sideris, and A. Hajimiri, "An ultrasensitive CMOS magnetic biosensor array with correlated double counting noise suppression," in *IEEE MTT-S Int. Microw. Symp. Dig.*, May 2010, pp. 616–619.
- [9] B. Eversmann *et al.*, "A  $128 \times 128$  CMOS biosensor array for extracellular recording of neural activity," *IEEE J. Solid-State Circuits*, vol. 38, no. 12, pp. 2306–2317, Dec. 2003.
- [10] M. K. Bhuyan, J. I. Rodriguez-Devora, K. Fraser, and T.-L. B. Tseng, "Silicon substrate as a novel cell culture device for myoblast cells," *J. Biomed. Sci.*, vol. 21, no. 1, p. 47, 2014.
- [11] N. J. Hallab, K. J. Bundy, K. O'Connor, R. L. Moses, and J. J. Jacobs, "Evaluation of metallic and polymeric biomaterial surface energy and surface roughness characteristics for directed cell adhesion," *Tissue Eng.*, vol. 7, no. 1, pp. 55–71, 2004.
- [12] T.-W. Chung, D.-L. Liu, S.-Y. Wang, and S.-S. Wang, "Enhancement of the growth of human endothelial cells by surface roughness at nanometer scale," *Biomaterials*, vol. 24, no. 25, pp. 4655–4661, 2003.
- [13] R. A. Gittens *et al.*, "The effects of combined micron-/submicron-scale surface roughness and nanoscale features on cell proliferation and differentiation," *Biomaterials*, vol. 32, no. 13, pp. 3395–3403, 2011.
- [14] I. Keen *et al.*, "Surface roughness and topography of poly(3-hydroxybutyrate-co-3-hydroxyvalerate) influences osteoblast cell growth," *J. Biomed. Sci.*, vol. 18, no. 9, pp. 1101–1123, 2007.
- [15] M. Jäger *et al.*, "Osteoblast differentiation onto different biomaterials with an endoprosthetic surface topography *in vitro*," *J. Biomed. Mater. Res.*, vol. 86A, no. 1, pp. 61–75, Jul. 2008.
- [16] H.-I. Chang and Y. Wang, "Cell responses to surface and architecture of tissue engineering scaffolds," in *Regenerative Medicine and Tissue Engineering—Cells and Biomaterials*, vol. 8, D. Eberli, Ed. Rijeka, Croatia: InTech, 2011, pp. 569–589.
- [17] J. S. Park *et al.*, "A multi-modality CMOS sensor array for cell-based assay and drug screening," in *Proc. IEEE ISSCC*, Feb. 2015, pp. 208–209.
- [18] H. S. Yang, C. Zhang, and M. S. Bakir, "Self-aligned silicon interposer tiles and silicon bridges using positive self-alignment structures and rematable mechanically flexible interconnects," *IEEE Trans. Compon., Packag., Manuf. Technol.*, vol. 4, no. 11, pp. 1760–1768, Nov. 2014.
- [19] C. Zhang, H. S. Yang, and M. S. Bakir, "Highly elastic gold passivated mechanically flexible interconnects," *IEEE Trans. Compon., Packag., Manuf. Technol.*, vol. 3, no. 10, pp. 1632–1639, Oct. 2013.
- [20] M. Zia *et al.*, "Fabrication of and cell growth on 'silicon membranes' with high density TSVs for bio-sensing applications," in *Proc. IEEE Biomed. Circuits Syst. Conf. (BioCAS)*, Atlanta, GA, USA, Oct. 2015, pp. 1–4.



**Muneeb Zia** (S'14) received the B.S. (Hons.) degree in electronic engineering from the Ghulam Ishaq Khan Institute of Engineering Sciences and Technology, Topi, Pakistan, in 2010, and the M.S. degree in electrical and computer engineering from the Georgia Institute of Technology, Atlanta, GA, USA, in 2013, where he is currently pursuing the Ph.D. degree in electrical and computer engineering.

His current research interests include fabrication and characterization of flexible interconnects and packaging for silicon photonics and biosensing platforms.



**Taiyun Chi** (S'11) received the B.S. degree (Hons.) from the University of Science and Technology of China, Hefei, China, in 2012. He is currently pursuing the Ph.D. degree in electrical engineering with the Georgia Institute of Technology, Atlanta, GA, USA.

His current research interests include millimeter-wave/terahertz integrated circuits and integrated biomedical sensors and actuators.

Mr. Chi was a recipient of the 2016 Microwave Theory and Techniques Society Graduate Fellowship for Medical Applications, a co-recipient of the IEEE Radio Frequency Integrated Circuits Symposium Best Student Paper Award (second place) in 2016, a recipient of the Analog Devices Inc. Outstanding Student Designer Award in 2015, and the Texas Instruments CICC Student Scholarship Award in 2014. He was also a recipient of the Georgia Tech GEDC Fellowship in 2012 and the USTC Guo Moruo Scholarship in 2012.

for Medical Applications

Evaluation of metallic and polymeric biomaterial surface energy and surface roughness characteristics for directed cell adhesion

Enhancement of the growth of human endothelial cells by surface roughness at nanometer scale

The effects of combined micron-/submicron-scale surface roughness and nanoscale features on cell proliferation and differentiation

Surface roughness and topography of poly(3-hydroxybutyrate-co-3-hydroxyvalerate) influences osteoblast cell growth

Osteoblast differentiation onto different biomaterials with an endoprosthetic surface topography *in vitro*

Cell responses to surface and architecture of tissue engineering scaffolds

A multi-modality CMOS sensor array for cell-based assay and drug screening

Self-aligned silicon interposer tiles and silicon bridges using positive self-alignment structures and rematable mechanically flexible interconnects

Highly elastic gold passivated mechanically flexible interconnects

Fabrication of and cell growth on 'silicon membranes' with high density TSVs for bio-sensing applications

for Medical Applications

Evaluation of metallic and polymeric biomaterial surface energy and surface roughness characteristics for directed cell adhesion

Enhancement of the growth of human endothelial cells by surface roughness at nanometer scale

The effects of combined micron-/submicron-scale surface roughness and nanoscale features on cell proliferation and differentiation

Surface roughness and topography of poly(3-hydroxybutyrate-co-3-hydroxyvalerate) influences osteoblast cell growth

Osteoblast differentiation onto different biomaterials with an endoprosthetic surface topography *in vitro*

Cell responses to surface and architecture of tissue engineering scaffolds

A multi-modality CMOS sensor array for cell-based assay and drug screening

Self-aligned silicon interposer tiles and silicon bridges using positive self-alignment structures and rematable mechanically flexible interconnects

Highly elastic gold passivated mechanically flexible interconnects

Fabrication of and cell growth on 'silicon membranes' with high density TSVs for bio-sensing applications

for Medical Applications

Evaluation of metallic and polymeric biomaterial surface energy and surface roughness characteristics for directed cell adhesion

Enhancement of the growth of human endothelial cells by surface roughness at nanometer scale

The effects of combined micron-/submicron-scale surface roughness and nanoscale features on cell proliferation and differentiation

Surface roughness and topography of poly(3-hydroxybutyrate-co-3-hydroxyvalerate) influences osteoblast cell growth

Osteoblast differentiation onto different biomaterials with an endoprosthetic surface topography *in vitro*

Cell responses to surface and architecture of tissue engineering scaffolds

A multi-modality CMOS sensor array for cell-based assay and drug screening

Self-aligned silicon interposer tiles and silicon bridges using positive self-alignment structures and rematable mechanically flexible interconnects

Highly elastic gold passivated mechanically flexible interconnects

Fabrication of and cell growth on 'silicon membranes' with high density TSVs for bio-sensing applications

for Medical Applications

Evaluation of metallic and polymeric biomaterial surface energy and surface roughness characteristics for directed cell adhesion

Enhancement of the growth of human endothelial cells by surface roughness at nanometer scale

The effects of combined micron-/submicron-scale surface roughness and nanoscale features on cell proliferation and differentiation

Surface roughness and topography of poly(3-hydroxybutyrate-co-3-hydroxyvalerate) influences osteoblast cell growth

Osteoblast differentiation onto different biomaterials with an endoprosthetic surface topography *in vitro*

Cell responses to surface and architecture of tissue engineering scaffolds

A multi-modality CMOS sensor array for cell-based assay and drug screening

Self-aligned silicon interposer tiles and silicon bridges using positive self-alignment structures and rematable mechanically flexible interconnects

Highly elastic gold passivated mechanically flexible interconnects

Fabrication of and cell growth on 'silicon membranes' with high density TSVs for bio-sensing applications

for Medical Applications

Evaluation of metallic and polymeric biomaterial surface energy and surface roughness characteristics for directed cell adhesion

Enhancement of the growth of human endothelial cells by surface roughness at nanometer scale

The effects of combined micron-/submicron-scale surface roughness and nanoscale features on cell proliferation and differentiation

Surface roughness and topography of poly(3-hydroxybutyrate-co-3-hydroxyvalerate) influences osteoblast cell growth

Osteoblast differentiation onto different biomaterials with an endoprosthetic surface topography *in vitro*

Cell responses to surface and architecture of tissue engineering scaffolds

A multi-modality CMOS sensor array for cell-based assay and drug screening

Self-aligned silicon interposer tiles and silicon bridges using positive self-alignment structures and rematable mechanically flexible interconnects

Highly elastic gold passivated mechanically flexible interconnects

Fabrication of and cell growth on 'silicon membranes' with high density TSVs for bio-sensing applications

for Medical Applications

Evaluation of metallic and polymeric biomaterial surface energy and surface roughness characteristics for directed cell adhesion

Enhancement of the growth of human endothelial cells by surface roughness at nanometer scale

The effects of combined micron-/submicron-scale surface roughness and nanoscale features on cell proliferation and differentiation

Surface roughness and topography of poly(3-hydroxybutyrate-co-3-hydroxyvalerate) influences osteoblast cell growth

Osteoblast differentiation onto different biomaterials with an endoprosthetic surface topography *in vitro*

Cell responses to surface and architecture of tissue engineering scaffolds

A multi-modality CMOS sensor array for cell-based assay and drug screening

Self-aligned silicon interposer tiles and silicon bridges using positive self-alignment structures and rematable mechanically flexible interconnects

Highly elastic gold passivated mechanically flexible interconnects

Fabrication of and cell growth on 'silicon membranes' with high density TSVs for bio-sensing applications

for Medical Applications

Evaluation of metallic and polymeric biomaterial surface energy and surface roughness characteristics for directed cell adhesion

Enhancement of the growth of human endothelial cells by surface roughness at nanometer scale

The effects of combined micron-/submicron-scale surface roughness and nanoscale features on cell proliferation and differentiation

Surface roughness and topography of poly(3-hydroxybutyrate-co-3-hydroxyvalerate) influences osteoblast cell growth

Osteoblast differentiation onto different biomaterials with an endoprosthetic surface topography *in vitro*

Cell responses to surface and architecture of tissue engineering scaffolds

A multi-modality CMOS sensor array for cell-based assay and drug screening

Self-aligned silicon interposer tiles and silicon bridges using positive self-alignment structures and rematable mechanically flexible interconnects

Highly elastic gold passivated mechanically flexible interconnects

Fabrication of and cell growth on 'silicon membranes' with high density TSVs for bio-sensing applications

for Medical Applications

Evaluation of metallic and polymeric biomaterial surface energy and surface roughness characteristics for directed cell adhesion

Enhancement of the growth of human endothelial cells by surface roughness at nanometer scale

The effects of combined micron-/submicron-scale surface roughness and nanoscale features on cell proliferation and differentiation

Surface roughness and topography of poly(3-hydroxybutyrate-co-3-hydroxyvalerate) influences osteoblast cell growth

Osteoblast differentiation onto different biomaterials with an endoprosthetic surface topography *in vitro*

Cell responses to surface and architecture of tissue engineering scaffolds

A multi-modality CMOS sensor array for cell-based assay and drug screening

Self-aligned silicon interposer tiles and silicon bridges using positive self-alignment structures and rematable mechanically flexible interconnects

Highly elastic gold passivated mechanically flexible interconnects

Fabrication of and cell growth on 'silicon membranes' with high density TSVs for bio-sensing applications

for Medical Applications

Evaluation of metallic and polymeric biomaterial surface energy and surface roughness characteristics for directed cell adhesion

Enhancement of the growth of human endothelial cells by surface roughness at nanometer scale

The effects of combined micron-/submicron-scale surface roughness and nanoscale features on cell proliferation and differentiation

Surface roughness and topography of poly(3-hydroxybutyrate-co-3-hydroxyvalerate) influences osteoblast cell growth

Osteoblast differentiation onto different biomaterials with an endoprosthetic surface topography *in vitro*

Cell responses to surface and architecture of tissue engineering scaffolds

A multi-modality CMOS sensor array for cell-based assay and drug screening

Self-aligned silicon interposer tiles and silicon bridges using positive self-alignment structures and rematable mechanically flexible interconnects

Highly elastic gold passivated mechanically flexible interconnects

Fabrication of and cell growth on 'silicon membranes' with high density TSVs for bio-sensing applications

for Medical Applications

Evaluation of metallic and polymeric biomaterial surface energy and surface roughness characteristics for directed cell adhesion

Enhancement of the growth of human endothelial cells by surface roughness at nanometer scale

The effects of combined micron-/submicron-scale surface roughness and nanoscale features on cell proliferation and differentiation

Surface roughness and topography of poly(3-hydroxybutyrate-co-3-hydroxyvalerate) influences osteoblast cell growth

Osteoblast differentiation onto different biomaterials with an endoprosthetic surface topography *in vitro*

Cell responses to surface and architecture of tissue engineering scaffolds

A multi-modality CMOS sensor array for cell-based assay and drug screening

Self-aligned silicon interposer tiles and silicon bridges using positive self-alignment structures and rematable mechanically flexible interconnects

Highly elastic gold passivated mechanically flexible interconnects

Fabrication of and cell growth on 'silicon membranes' with high density TSVs for bio-sensing applications

for Medical Applications

Evaluation of metallic and polymeric biomaterial surface energy and surface roughness characteristics for directed cell adhesion

Enhancement of the growth of human endothelial cells by surface roughness at nanometer scale

The effects of combined micron-/submicron-scale surface roughness and nanoscale features on cell proliferation and differentiation

Surface roughness and topography of poly(3-hydroxybutyrate-co-3-hydroxyvalerate) influences osteoblast cell growth

Osteoblast differentiation onto different biomaterials with an endoprosthetic surface topography *in vitro*

Cell responses to surface and architecture of tissue engineering scaffolds

A multi-modality CMOS sensor array for cell-based assay and drug screening

Self-aligned silicon interposer tiles and silicon bridges using positive self-alignment structures and rematable mechanically flexible interconnects

Highly elastic gold passivated mechanically flexible interconnects

Fabrication of and cell growth on 'silicon membranes' with high density TSVs for bio-sensing applications

for Medical Applications

Evaluation of metallic and polymeric biomaterial surface energy and surface roughness characteristics for directed cell adhesion

Enhancement of the growth of human endothelial cells by surface roughness at nanometer scale

The effects of combined micron-/submicron-scale surface roughness and nanoscale features on cell proliferation and differentiation

Surface roughness and topography of poly(3-hydroxybutyrate-co-3-hydroxyvalerate) influences osteoblast cell growth

Osteoblast differentiation onto different biomaterials with an endoprosthetic surface topography *in vitro*

Cell responses to surface and architecture of tissue engineering scaffolds

A multi-modality CMOS sensor array for cell-based assay and drug screening

Self-aligned silicon interposer tiles and silicon bridges using positive self-alignment structures and rematable mechanically flexible interconnects

Highly elastic gold passivated mechanically flexible interconnects

Fabrication of and cell growth on 'silicon membranes' with high density TSVs for bio-sensing applications

for Medical Applications

Evaluation of metallic and polymeric biomaterial surface energy and surface roughness characteristics for directed cell adhesion

Enhancement of the growth of human endothelial cells by surface roughness at nanometer scale

The effects of combined micron-/submicron-scale surface roughness and nanoscale features on cell proliferation and differentiation

Surface roughness and topography of poly(3-hydroxybutyrate-co-3-hydroxyvalerate) influences osteoblast cell growth

Osteoblast differentiation onto different biomaterials with an endoprosthetic surface topography *in vitro*

Cell responses to surface and architecture of tissue engineering scaffolds

A multi-modality CMOS sensor array for cell-based assay and drug screening

Self-aligned silicon interposer tiles and silicon bridges using positive self-alignment structures and rematable mechanically flexible interconnects

Highly elastic gold passivated mechanically flexible interconnects

Fabrication of and cell growth on 'silicon membranes' with high density TSVs for bio-sensing applications

for Medical Applications

Evaluation of metallic and polymeric biomaterial surface energy and surface roughness characteristics for directed cell adhesion

Enhancement of the growth of human endothelial cells by surface roughness at nanometer scale

The effects of combined micron-/submicron-scale surface roughness and nanoscale features on cell proliferation and differentiation

Surface roughness and topography of poly(3-hydroxybutyrate-co-3-hydroxyvalerate) influences osteoblast cell growth

Osteoblast differentiation onto different biomaterials with an endoprosthetic surface topography *in vitro*

Cell responses to surface and architecture of tissue engineering scaffolds

A multi-modality CMOS sensor array for cell-based assay and drug screening

Self-aligned silicon interposer tiles and silicon bridges using positive self-alignment structures and rematable mechanically flexible interconnects

Highly elastic gold passivated mechanically flexible interconnects

Fabrication of and cell growth on 'silicon membranes' with high density TSVs for bio-sensing applications

for Medical Applications

Evaluation of metallic and polymeric biomaterial surface energy and surface roughness characteristics for directed cell adhesion

Enhancement of the growth of human endothelial cells by surface roughness at nanometer scale

The effects of combined micron-/submicron-scale surface roughness and nanoscale features on cell proliferation and differentiation

Surface roughness and topography of poly(3-hydroxybutyrate-co-3-hydroxyvalerate) influences osteoblast cell growth

Osteoblast differentiation onto different biomaterials with an endoprosthetic surface topography *in vitro*

Cell responses to surface and architecture of tissue engineering scaffolds

A multi-modality CMOS sensor array for cell-based assay and drug screening

Self-aligned silicon interposer tiles and silicon bridges using positive self-alignment structures and rematable mechanically flexible interconnects

Highly elastic gold passivated mechanically flexible interconnects

Fabrication of and cell growth on 'silicon membranes' with high density TSVs for bio-sensing applications

for Medical Applications

Evaluation of metallic and polymeric biomaterial surface energy and surface roughness characteristics for directed cell adhesion

Enhancement of the growth of human endothelial cells by surface roughness at nanometer scale

The effects of combined micron-/submicron-scale surface roughness and nanoscale features on cell proliferation and differentiation

Surface roughness and topography of poly(3-hydroxybutyrate-co-3-hydroxyvalerate) influences osteoblast cell growth

Osteoblast differentiation onto different biomaterial



**Mark P. Styczynski** received the B.S. degree in chemical engineering from the University of Notre Dame, Notre Dame, IN, USA, in 2002, and the Ph.D. degree in chemical engineering from the Massachusetts Institute of Technology, Cambridge, MA, USA, in 2007.

From 2007 to 2009, he was a Post-Doctoral Fellow at the Broad Institute, Cambridge. In 2009, he was an Assistant Professor with the School of Chemical and Biomolecular Engineering, Georgia Institute of Technology, Atlanta, GA, USA. He was an NSF Graduate Research Fellow and NIH Ruth L. Kirschstein NRSA Post-Doctoral Fellow during his doctoral work and post-doctoral training, respectively.

Dr. Styczynski was a recipient of the DARPA Young Faculty Award and the Ralph E. Powe Junior Faculty Enhancement Award from Oak Ridge Associated Universities in 2011. In 2013, he was a recipient of the NSF CAREER Award. He has also received numerous department and institution-level teaching awards.



**Hua Wang** (M'05–SM'15) received the M.S. and Ph.D. degrees in electrical engineering from the California Institute of Technology, Pasadena, CA, USA, in 2007 and 2009, respectively.

He was with Intel Corporation, Hillsboro, OR, USA, and Skyworks Solutions, San Jose, CA, USA. He joined the School of Electrical and Computer Engineering, Georgia Institute of Technology, Atlanta, GA, USA, as an Assistant Professor in 2012. His current research interests include mixed-signal, RF, and millimeter-wave integrated systems

for wireless communication and bioelectronics applications.

Dr. Wang was a recipient of the 2015 National Science Foundation CAREER Award, the 2016 Georgia Tech Sigma Xi Young Faculty Award, the 2014 DURIP Award, the 2015 Georgia Tech ECE Outstanding Junior Faculty Member Award, and the 2015 Lockheed Dean's Excellence in Teaching Award. He currently holds the Demetrius T. Paris Junior Professorship of the School of Electrical and Computer Engineering. His research group Georgia-Tech Electronics and Micro-System laboratory has won multiple student paper awards and student designer awards, including the IEEE RFIC Best Student Paper Awards in 2014 (first place) and 2016 (second place), the 2016 *IEEE Microwave Magazine* Best Paper Award, IEEE CICC Best Student Paper Finalists thrice, and the Analog Devices Outstanding Student Designer Awards four times. He is an Associate Editor of the IEEE MICROWAVE AND WIRELESS COMPONENTS LETTERS. He is currently a Technical Program Committee Member for the IEEE Radio Frequency Integrated Circuits Symposium, the IEEE Custom Integrated Circuits Conference, the IEEE Bipolar/BiCMOS Circuits and Technology Meeting, and the IEEE Biomedical Circuits and Systems Conference. He is a member of Sigma Xi, the IEEE Solid-State Circuits Society, the IEEE Microwave Theory and Techniques Society, the IEEE Circuits and Systems Society, and the IEEE Engineering in Medicine & Biology Society. He serves as the Chair of the Atlanta's IEEE CAS/SSCS joint chapter, which won the IEEE SSCS Outstanding Chapter Award in 2014.



**Muhammed S. Bakir** (S'98–M'03–SM'12) received the B.E.E. degree from Auburn University, Auburn, AL, USA, in 1999, and the M.S. and Ph.D. degrees in electrical and computer engineering from the Georgia Institute of Technology (Georgia Tech), Atlanta, GA, USA, in 2000 and 2003, respectively.

He is currently a Professor with the School of Electrical and Computer Engineering, Georgia Tech. His current research interests include 3-D electronic system integration, advanced cooling and power delivery for 3-D systems, biosensors and their integration with CMOS circuitry, and nanofabrication technology.

Dr. Bakir was a recipient of the 2013 Intel Early Career Faculty Honor Award, the 2012 DARPA Young Faculty Award, and the 2011 IEEE CPMT Society Outstanding Young Engineer Award, and was an Invited Participant in the 2012 National Academy of Engineering Frontiers of Engineering Symposium. In 2015, he was elected by the IEEE CPMT Society to serve as a Distinguished Lecturer. He and his research group have received more than 20 conference and student paper awards, including five from the IEEE Electronic Components and Technology Conference, four from the IEEE International Interconnect Technology Conference, and one from the IEEE Custom Integrated Circuits Conference. His group was a recipient of the 2014 Best Paper of the IEEE TRANSACTIONS ON COMPONENTS, PACKAGING, AND MANUFACTURING TECHNOLOGY in the area of advanced packaging. He is an Editor of the IEEE TRANSACTIONS ON ELECTRON DEVICES and an Associate Editor of the IEEE TRANSACTIONS ON COMPONENTS, PACKAGING, AND MANUFACTURING TECHNOLOGY.